Applied Science and Innovative Research
ISSN 2474-4972 (Print) ISSN 2474-4980 (Online)
Vol. 9, No. 2, 2025
www.scholink.org/ojs/index.php/asir

Original Paper

Design and Parameter Optimization Analysis of the Tong Dies of the Clamping tong for the Iron Roughneck

Yongbai Sha[1*], Donghe Han[1], Kangshuai Yang[1], Xiaoying Zhao[2], Baihan Su[3] & Congzhi Liu[1]

[1] Key Laboratory of CNC Equipment Reliability, Ministry of Education, School of Mechanical and Aerospace Engineering, Jilin University, Changchun 130025, China

[2] Changchun Polytechnic University, Changchun 130033, China

[3] Gongzhuling Changchun XI High School Silicon Valley School, Changchun 136100, China

[*] Corresponding Author: Yongbai Sha, E-mail: shayb@jlu.edu.cn

Abstract

The clamping tong is a key component of the iron roughneck. During the work process, the tong dies of the clamping tong contact with the drilling tool directly and bear a significant force. The quality of the tong dies has a significant impact on both the operational efficiency of the iron roughneck and the service life of the tubular components it engages with. This paper, based on the actual working conditions of the tong dies, designs the clamping tong for iron roughneck, and focus on tooth profile analysis and parameter optimization of the tong dies. The contact between the tong dies and the drill string is studied, and the equivalent friction coefficient as well as the necessary conditions to prevent slippage are calculated. Additionally, the biting depth and biting conditions of the tong dies are computed. Finally, using the orthogonal experimental method, the correlation between four factors and the equivalent friction coefficient is established, and the optimal value range for these factors is determined. The paper concludes with a simulation-based analysis to identify the optimal parameters for the tong dies.

Keywords

iron roughneck, clamping tong, tong dies, mechanical analysis, tooth profile analysis, strength analysis, orthogonal experimental method

1. Introduction

The iron roughneck is a multifunctional, safe, and efficient drilling tool make-up and breakout device, and is an important auxiliary equipment in automated drilling systems in oilfields. The clamping tong is a key component of the iron roughneck. The tong dies of the clamping tong are contact with the drilling tool directly, bearing a large force and easily damaged. Frequent replacement of the tong dies will directly affect the work efficiency of the iron roughneck, and Unreasonable design of tong dies can directly affect the service life of the drilling tools in contact with them. Since the tong dies are a consumable part, in

order to extend their service life, it is necessary to improve the contact state between the tong dies and the drilling tool, increase the strength of the tong dies, and overcome the wear and breakage of the die teeth during the make-up and breakout operations.

Currently, Yancheng Teda Drilling & Production Equipment Co., Ltd. has developed a friction-type tong die. This friction-type tong die enables the make-up and breakout of tubing without causing damage to the tubing. However, it accelerates the wear of the friction material, leading to frequent replacements of the friction elements, which, to some extent, reduces the operational efficiency of the iron roughneck. Great Wall Drilling Engineering Co., Ltd. has developed a tooth-mark-free friction-type tong die. This new type of tong die addresses the issue of tooth marks caused by the tong dies on drill pipes and other tubular components during use, causing minimal damage to the drill pipes and extending their service life. However, its application is limited to low-torque situations, significantly restricting its usage range. The Institute of Metal Research, Chinese Academy of Sciences, has developed a composite oil drilling large tong die. This tong die consists of a base plate and composite teeth. The base plate is made from high-toughness structural steel, and the teeth are made from metal matrix composite materials. The teeth can be designed in straight-line, curved, or patterned structures. The tooth plate and teeth are bonded together through diffusion welding. After diffusion welding, the transition layer has a higher concentration of alloy elements. By subjecting the base material to tempering treatment, the strength of the material is improved, ensuring that it does not crack during use. Its wear resistance is several times higher than steel. The advantage of this tong die is its greatly increased service life and significantly reduced overall cost. However, during the make-up and breakout process, it is prone to causing larger tooth marks on drill pipes and other tubular components.

Although the tong dies of the iron roughneck are relatively well-developed, they still have the following issues: The load distribution between the tong dies and the drilling tool is uneven, stress concentration is likely to occur under the influence of clamping force and torque during operation. This can result in tooth marks on the surface of the drilling tool and damaging it, accelerating wear on the tong dies and reducing the service life of both the tong dies and the drilling tool. Therefore, it is necessary to conduct an analysis from the perspectives of the tong dies' geometry, overall load-bearing conditions, and wear patterns.

The tong dies are studied from the following aspects in this paper: material selection, tooth profile analysis, mechanical analysis, and contact condition analysis. Based on this, with the objective of achieving less than 1.2mm tooth marks on the drill string, longer service life of the tong dies, and providing greater torque, an orthogonal experiment is conducted to investigate the relationship between various parameters of the tong dies and the friction coefficient, in order to identify the optimal parameters. Finally, simulation experiments are conducted to analyze and determine the best parameters for the tong dies.

2. Structure of the Clamping Tong and Material of the Tong Dies plate

In the work of the iron roughneck, the first step is to extend and clamp the drilling tool with the clamping tong on both sides under the action of driving force, and then perform subsequent drilling tool make-up and breakout operations. The tong dies of the clamping tong contact with the drilling tool directly, and after long-term operation, they may fail due to wear on the tooth surface, brittle fracture of the tooth root, and other reasons, and cannot meet the normal working requirements, making them vulnerable parts. Therefore, the design of clamping tong should optimize the structure and parameters of the tong dies, thereby increasing the service life of the tong dies and reducing damage to the drilling tools. On the other hand, it is necessary to consider the ease of replacement after the tong dies wear out. Based on this usage requirement, the designed clamping tong structure is shown in Figure 1.

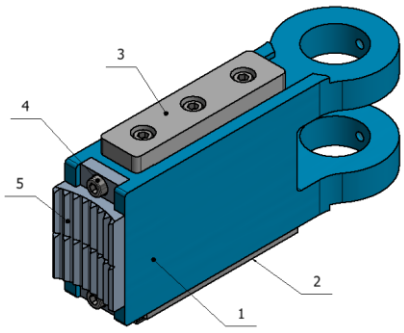

1. Base, 2. Lower guide rail, 3. Upper guide rail, 4. Screw, 5. tong dies plate

Figure 1. Structure of Clamping Tong

The clamping tong consists of a base, a lower guide rail, an upper guide rail, screws, and a tong dies plate. The upper and lower guide rails play a guiding role when the clamping tong extends and retracts. The front end of the base has a groove for positioning the tong dies plate, and the tong dies plate is connected to the base with screws. The tong dies front end face of the tong dies plate is designed as an arc-shaped structure, and the radius of this arc is the same as the radius of the clamped drilling tool. When working, select the matching tong dies plate according to the specifications of the drilling tools, so as to ensure that the contact surface between the tong dies and the drilling tools reaches the maximum, thereby improving the stress state. The groove structure and screw connection method at the front end of the base ensure the installation accuracy and good stress state of the tong dies plate, while also facilitating the replacement of the tong dies plate.

The tong dies of the clamping tong pliers bear significant forces in working engineering and is vulnerable parts. Therefore, while ensuring work efficiency, the frequency of replacement should be minimized as much as possible. Considering various factors, 20CrMnTi is selected as the material for the tong dies plate.

3. Analysis of the Tooth Profile of Tong Dies

3.1 Mechanical Analysis of the Tong Die Tooth Profile Angle

This paper selects tong dies of the clamping tong as the research object and conducts a mechanical analysis of the tooth profile angle. A cross-sectional diagram of the tong die is shown in Figure 2, where surface AC represents the front face of the tooth, AB represents the rear face, α_1 is the front angle of the tooth, α_2 is the rear angle of the tooth, β is the top angle of the tooth, h is the tooth height, and L is the thickness of the tong die tooth plate. During the breakout process, under the action of the clamping force, the tooth tip applies a normal pressure to the surface of the drilling tool. The tong die also transmits the breakout torque to the drilling tool through friction. At this moment, the tong die experiences a reaction force from the drilling tool. P represents the radial pressure acting on the tong die, and Q represents the tangential friction force acting on the tong die.

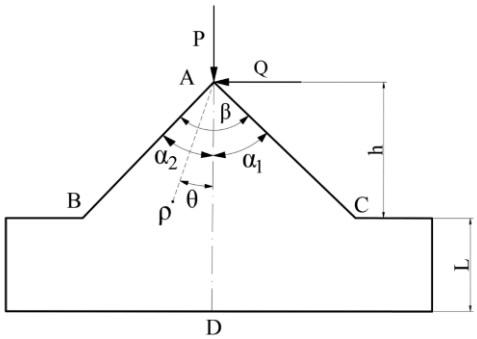

Figure 2. Cross-sectional Diagram of the Tong Die

The study of the force condition of the tong dies of the clamping tong falls under the force problem of the wedge angle in elastic mechanics. By applying Michel's solution, the force conditions of any point (ρ, θ) within the cross-section of the tong die in polar coordinates, with the tip of the tooth (point A) as the origin and the line AD as the polar axis, can be obtained as follows:

$$\begin{cases} \sigma_\rho = -\dfrac{2}{\rho}\left(\dfrac{P\cos\theta}{\beta+\sin\beta}+\dfrac{Q\sin\theta}{\beta-\sin\beta}\right) \\ \sigma_\theta = 0 \\ \tau_{\rho\theta} = \tau_{\theta\rho} = 0 \end{cases} \tag{1}$$

In the equation, σ_ρ represents radial stress; σ_θ represents tangential stress; $\tau_{\rho\theta}$ represents shear stress on the radial-tangential plane; $\tau_{\theta\rho}$ represents shear stress on the tangential-radial plane.

If the stresses on both sides of the tong dies of the clamping tong are made equal, when the direction of the polar axis coincides with the bisector of the tooth apex angle, then we have $\sigma_\rho(\theta) = \sigma_\rho(-\theta)$. Substituting this into equation (1) gives:

$$\frac{Q\sin\theta}{\beta-\sin\beta}=0 \tag{2}$$

Given $\beta \neq 0$ and $\sin\theta \neq 0$, equation (2) is always valid when $Q = 0$ is considered. At this point, the stress conditions on both sides of the tooth apex bisector of the tong die are identical. Since the tong die only experiences radial pressure P, the resultant force of the radial force P and tangential force Q is simply the radial pressure P. As the direction of the radial force P coincides with the direction of the polar axis AD, and the direction of the polar axis coincides with the bisector of the tooth apex angle, the direction of the radial force P coincides with the bisector of the tooth apex angle as well. This means that when the resultant force of the radial pressure P and the tangential frictional force Q aligns with the bisector of the tooth apex angle, the stresses on both sides of the tong die are the same. Under this structural arrangement, the internal stress distribution of the tooth body is uniform, which is more favorable for the tong die to perform its function.

During the tonging process, the radial pressure P and the tangential frictional force Q are not constant. As the upper tong body rotates and the tightness between the drilling tool threads changes, the radial and tangential forces will also vary. Furthermore, the direction of the resultant force of the radial and tangential forces will change due to slight wear on the tooth tip during operation. Therefore, it is impossible to ensure that the direction of the resultant force on the tong die always aligns with the bisector of the tooth apex angle. If the resultant force on the tong die remains within a certain range, such that the direction of the tooth apex bisector falls within the range of the resultant force's angle, it can ensure that the direction of the bisector is as close as possible to the direction of the resultant force, thereby making the stress distribution on both sides of the tong die approximately the same.

Under the assumption that the tong die is not embedded into the drilling tool, since the radial force P is a compressive force and the tangential force Q is a frictional force, their ratio is the coefficient of friction f, i.e., $f = Q / P = \tan\varphi$, where φ is the friction angle. Typically, the coefficient of friction between the tong dies and the drilling tool, without lubrication, is denoted as $f \in$ (0.15, 0.3), and in this study, the static friction coefficient is denoted as f=0.15. After determining the tooth apex angle β, the tooth front angle $\alpha_1 = \beta/2 - \varphi$ and the tooth back angle $\alpha_2 = \beta/2 + \varphi$ can be obtained. However, during the tonging process, there will be a significant tonging torque and clamping force, causing the tong die to embed into the drilling tool. At this point, the coefficient of friction f will increase, which in turn increases the friction angle φ. Consequently, the tooth front angle will decrease, and the tooth back angle will increase. Regardless of whether the tong die is embedded into the drilling tool, the stress requirements must be met for the tooth body. Therefore, when designing the tooth front angle, the impact of the friction angle on the tooth apex angle in the non-embedded state is the primary factor, while when designing the tooth back angle, the effect of the friction angle in the embedded state on the tooth apex angle is the main consideration.

3.2 Calculation of Tong Die Height

The main basis for calculating the height of the tong die is to ensure that the root of the tong die reaches

the required strength. When the tooth front angle and tooth back angle of the tong die are the same, the greater the height of the tong die, the greater the stress on the front and back faces of the tooth. In this case, the stress distribution decreases gradually from the tooth tip to the tooth root. Since the stress distribution is uneven, it is particularly important to analyze the height of the tong die. The height of the tong die is denoted as h. In the established polar coordinate system, the stress at the root of the tooth can be expressed as:

$$\sigma_\rho = -\frac{2}{\rho}\left(\frac{P\cos\theta}{\beta+\sin\beta}+\frac{Q\sin\theta}{\beta-\sin\beta}\right) \tag{3}$$

Based on the cross-sectional diagram of the tong die, the relationship between θ and h can be expressed as:

$$y = \rho\cos\theta = -h \tag{4}$$

By solving equations (3) and equations (4) simultaneously, the following can be obtained:

$$\sigma_\rho = \frac{2h}{\rho^2}\left[\frac{P}{\beta+\sin\beta}+\frac{Q\sqrt{\rho^2-h^2}}{h(\beta-\sin\beta)}\right] \le \left[\sigma_\rho\right] \tag{5}$$

The result can be organized as follows:

$$\sigma_\rho = \frac{2hP}{\rho^2(\beta+\sin\beta)}+\frac{2Q\sqrt{\rho^2-h^2}}{\rho^2(\beta-\sin\beta)} = \sigma_1+\sigma_2 \le \left[\sigma_\rho\right] \tag{6}$$

Where:

$$\sigma_1 = \frac{2h}{\rho^2(\beta+\sin\beta)}P \tag{7}$$

$$\sigma_2 = \frac{2\sqrt{\rho^2-h^2}}{\rho^2(\beta-\sin\beta)}Q = \frac{2}{\beta-\sin\beta}\sqrt{\frac{1}{\rho^2}-\frac{h^2}{\rho^4}}Q \tag{8}$$

In the equation, σ_1 represents the vertical stress at the root of the tong die; σ_2 represents the horizontal stress at the root of the tong die.

Where the domains of θ and ρ are defined as: $\theta \in (\alpha_2, \alpha_1)$, $\rho \in (-h\cos\alpha_2, -h\cos\alpha_1)$.

In equation (8), let $m = \frac{1}{\rho^2}-\frac{h^2}{\rho^4}, n = \frac{1}{\rho^2}$, then we have:

$$m = n - n^2h^2 \tag{9}$$

By differentiating equation (9) with respect to n, we get:

$$\frac{dm}{dn} = 1-2h^2n \tag{10}$$

Let equation (10) equal 0, then a achieves $n = 1/2h^2$ maximum value at:

$$m = \frac{1}{2h^2}-\frac{h^2}{4h^4} = \frac{1}{4h^2} \tag{11}$$

Through calculations, it is found that the stress on the root of the tong die mainly comes from radial and tangential loads. The magnitude of the stress increases with the increase in radial and tangential loads,

and the coefficients are related to the height of the tong die h. From equation (7), it can be concluded that when the radial force P is fixed, σ_1 is proportional to the height of the tong die h, and σ_1 is the main component of the stress on the tooth root. At different positions along the tooth root ρ, the radial stress will change, with the maximum vertical stress on the entire tooth root occurring at point $\rho = h$. From equation (8) to equation (11), it can be concluded that when the tangential force Q is fixed, σ_2 decreases with the increase of the tong die height h. At different positions along the tooth root ρ, the tangential stress will change, with the maximum horizontal stress on the entire tooth root occurring at point $\rho = \sqrt{2}h$. Therefore, the maximum radial stress and maximum tangential stress at the tooth root must both meet the design requirements, which can then be used to calculate the range of the tong die height h.

4. Analysis of the Contact Conditions Between the Tong Die and the Drilling tool

When the tong die of the clamping tong comes into contact with the drilling tool, under the action of the clamping force, the tong die will undergo slight deformation. To simplify the analysis, the theoretical model must satisfy the following two assumptions: Both the tong die of the clamping tong and the drilling tool are elastic bodies, and the elastic deformations that occur during the tonging process are assumed to be small. The tong die of the clamping tong is symmetrically distributed on both sides of the drilling tool, and the drilling tool itself has symmetry. Environmental factors are not considered, and the stress conditions on both sides of the tong die and the drilling tool are assumed to be the same.

4.1 Equivalent Coefficient of Friction and Anti-Slip Conditions

During tonging, a straight-tooth tong die is selected. Since the tong die is used to grip the drilling tool and provide torque, a vertical tooth tong die is chosen, which is parallel to the axis of the drilling tool. The schematic diagram of the cross-sectional view of the tong die clamping the drilling tool during the tonging process is shown in Figure 3:

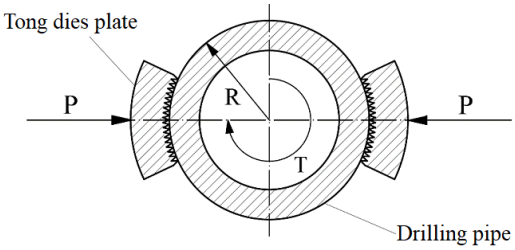

Figure 3. Schematic of Clamping State

During the entire tonging process, under the action of the clamping hydraulic cylinder, the tong die is moved toward the drilling tool until the tip of the tong die contacts the outer wall of the drilling tool. The clamping hydraulic cylinder maintains the oil pressure, which is transmitted to the tong die as radial force P. Afterward, the tonging hydraulic cylinder operates, generating the tonging torque T. At this point, the

torque T is transmitted to the drilling tool through the frictional force generated between the tong die and the drilling tool. When the tong die bites into the outer wall of the drilling tool, the structural diagram is shown in Figure 4.

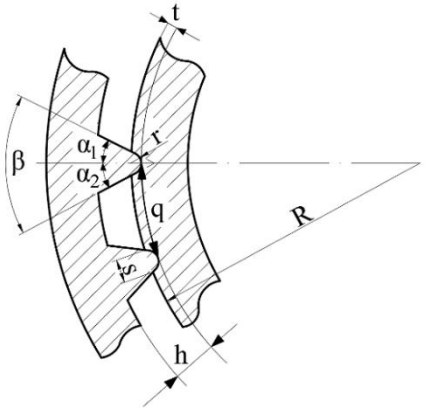

Figure 4. Structural Diagram of Biting State

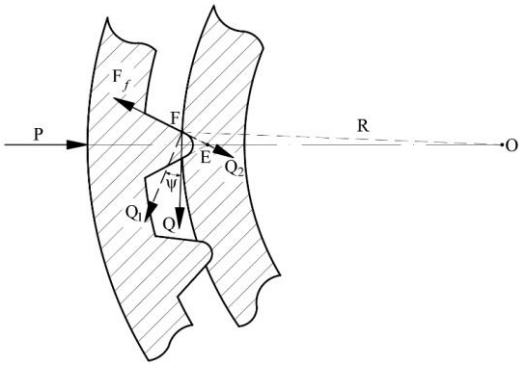

Figure 5. Force Analysis Diagram

According to Figure 4, it can be seen that: α_1 is the tooth front angle, α_2 is the tooth back angle, β is the tooth apex angle, R is the radius at the drilling tool joint, r is the radius of the transition curve of the tooth apex angle, t is the depth at which the tong die bites into the drilling tool, s is the width of the tong die's bite into the drilling tool, h is the height of the tong die, q is the circumferential distance between the tips of the two tong dies. Since make-up and break-out are inverse processes, the tooth front angle during make-up is equal to the tooth back angle during break-out, so it can be inferred that $\alpha_1 = \alpha_2 = \beta/2$. At this point, the cross-section of the tong die is an isosceles triangle. The tangential force Q exerted by the tong die on the drilling tool is used to transmit the torque T. The lever arm of the tangential force acting on the drilling tool is calculated as the minimum value $R - t$. If the number of the tong die teeth is m, the expression for the tangential force Q is:

$$Q = \frac{T}{m(R-t)} \tag{12}$$

From a microscopic perspective, during the tonging process, the tong die bites into the surface of the drilling tool. At this point, compressive pressure is generated between the front face of the tong die and the drilling tool to transmit the torque, and frictional forces exist between the contact surfaces. Taking the clockwise torque generated by the tonging hydraulic cylinder as an example, the force conditions between the tong die and the drilling tool are shown in Figure 5.

In Figure 5, P is the normal pressure transmitted to the tong die by the clamping hydraulic cylinder, Q is the tangential force between the tong die and the drilling tool, and F_f is the frictional force between the contact surfaces. The tangential force Q is decomposed into two components: one along the direction of the frictional force and the other perpendicular to it. These components are Q_1, which is the component perpendicular to the contact surface, and Q_2, which is the component along the contact surface. The angle

between Q_1 and Q is denoted as ψ.

Based on the force balance, the expression for the frictional force F_f can be obtained as:

$$F_f = Q_1 f \tag{13}$$

In the equation, f is the coefficient of friction between the front face of the tong die and the surface of the drilling tool. Here, $f = 0.2$.

Where the relationship between the component force Q_1 and the tangential force Q is:

$$Q_1 = Q\cos\angle OFE \tag{14}$$

In $\triangle OEF$, the sine formula can be used to obtain:

$$\frac{R}{\sin\angle FEO} = \frac{OE}{\sin\angle OFE} \tag{15}$$

Further simplification leads to:

$$\sin\angle OFE = \frac{OE}{R}\sin\alpha_1 \tag{16}$$

Where $OE = R + r - t - r/\sin\alpha_1$, when substituted into equation (16), gives:

$$\sin\angle OFE = \frac{R + r - t - \dfrac{r}{\sin\alpha_1}}{R}\sin\alpha_1 = \frac{\sin\alpha_1\left(R + r - t\right) - r}{R} \tag{17}$$

From Figure 5, it can be seen that $\angle OFE = \psi$, and thus the expression for the component force Q_1 perpendicular to the contact surface, can be obtained as:

$$Q_1 = Q\cos\psi = \frac{T}{m\left(R - t\right)}\sqrt{1 - \frac{\left[\sin\alpha_1\left(R + r - t\right) - r\right]^2}{R^2}} \tag{18}$$

Since during the tonging process, the tong die continuously grips the drilling tool, and the two remain in a relatively stationary state, the overall force balance can be established. Based on the mechanical relationships, the following can be obtained:

$$\begin{cases} P = Q\sin\angle FOE + F_f\cos\alpha_1 \\ Q\cos\angle FOE = F_f\sin\alpha_1 \end{cases} \tag{19}$$

Further simplification leads to:

$$\begin{cases} \sin\angle FOE = \dfrac{P}{Q} - f\cos\psi\cos\alpha_1 \\ \cos\angle FOE = f\cos\psi\sin\alpha_1 \end{cases} \tag{20}$$

Where $f_v = Q/P$, and f_v is the equivalent coefficients of friction when the tong die comes into contact with the drilling tool, and their expression is:

$$f_v = \frac{1}{f\cos\alpha_1\sqrt{1 - \dfrac{\left[\sin\alpha_1\left(R + r - t\right) - r\right]^2}{R^2}} + \sqrt{1 - f^2\sin^2\alpha_1\left\{1 - \dfrac{\left[\sin\alpha_1\left(R + r - t\right) - r\right]^2}{R^2}\right\}}} \tag{21}$$

Based on the relationship between the clamping force P and the tonging torque T, the following can be obtained:

$$T = Pf_v\left(R-t\right) \tag{22}$$

To ensure that no slipping occurs between the tong die and the drilling tool during the tonging process, and that they remain in a relatively stationary state, a sufficiently large clamping force is required so that the frictional torque exceeds the tonging resistance torque. This will meet the practical working requirements. In other words, the clamping force P should satisfy the following relationship:

$$P \geq \frac{T}{\left(R-t\right) f_v} \tag{23}$$

Only when the clamping force P satisfies equation (23) can the tonging action be successfully carried out. If the tip of the tong dies experiences wear, the equivalent coefficient of friction f_v will decrease, requiring a larger clamping force to meet the working requirements. Otherwise, slippage may occur, leading to further damage to both the tong die and the drilling tool surfaces. Therefore, since the tong die is a vulnerable component, it should be regularly replaced to prevent slippage from occurring.

4.2 Tong Die Insertion Depth and Insertion Conditions

During the process of clamping the drilling tool, the tong die will bite into the surface of the drilling tool. At this point, both the tong die and the drilling tool surface will undergo elastic and plastic deformations sequentially. When the tong die first contacts the surface of the drilling tool, elastic deformation occurs. As the clamping force increases, the tip of the tong die and the surface material of the drilling tool gradually reach the limit stress, causing yielding in the contact area of the metal material, which results in plastic deformation. As the depth of the tong die biting into the drilling tool surface increases, the contact area between the tong dies and the drilling tool surface continues to grow. When the generated tangential frictional torque is sufficient to overcome the tonging resistance torque, the tong die stops biting further into the drilling tool, reaching a state of equilibrium. The insertion depth t can be calculated based on the yielding degree of the tong die's clamping part. According to Figure 4, it can be seen that:

$$\begin{cases} s = 2r\sin\left(90°-\alpha_1\right) \\ t = r - r\cos(90-\alpha_1) \end{cases} \tag{24}$$

Where $\alpha_1 = \alpha_2 = \beta/2$, further simplification leads to:

$$t = \frac{s}{2\cos\alpha_1} - \frac{s\tan\alpha_1}{2} = \frac{s}{2}\left(\frac{1}{\cos\alpha_1} - \tan\alpha_1\right) \tag{25}$$

In the model of the tong die engaging with the drilling tool, there exists:

$$\frac{P}{kmls} = \left[\sigma_s\right] \tag{26}$$

In the equation, $[\sigma_s]$ is the yield strength of the material of the outer wall of the drilling tool, and k is the safety factor, and m is the total number of tong die teeth, and l is the length of each tong die along the axis of the drilling tool, and s is the width of the tong die's bite into the drilling tool.

By combining equation (25) and equation (26), the insertion depth t can be obtained as:

$$t = \frac{P}{2kml[\sigma_s]}\left(\frac{1}{\cos\alpha_1} - \tan\alpha_1\right) \tag{27}$$

The stress generated by the clamping force P on the extrusion surface between the tong die and the drilling tool is:

$$\sigma_P = \frac{P}{mA_p} \tag{28}$$

To ensure that the tip of the tong die can bite into the surface of the drilling tool, the clamping force P needs to satisfy the following relationship:

$$P \geq 2ml[\sigma_s]\sqrt{\left(1 - f^2\sin^2\alpha_1\right)R^2 + f^2\sin^2\alpha_1\left[\sin\alpha_1\left(R + r - t\right) - r\right]^2} \tag{29}$$

Where $[\sigma_s]$ is the allowable yield strength of the material of the outer wall of the drilling tool.

5. Orthogonal Experiment of the Tong Die of the Clamping tong

During the process of the tong die of the clamping tong clamping the drilling tool, as derived from equation (21), the equivalent coefficient of friction f_v, which determines the contact effect between the tong die and the drilling tool surface, is influenced by multiple variables, including the bite depth t, the tooth apex radius r, the tooth front angle α_1, and the radius at the drilling tool joint R. To determine the optimal parameter combination, an orthogonal experiment is conducted for analysis. The design of the orthogonal experiment involves four influencing factors, each with four different levels, as shown in Table 1. By arranging and combining the different levels of these factors, and systematically evaluating the impact of different combinations on the equivalent coefficient of friction, the best parameter combination can be identified to increase the equivalent friction coefficient and improve the contact effect between the tong die and the drilling tool.

Table 1. Orthogonal Experiment Factors and Levels Distribution

Factor Sign	Bite Depth t (mm)	Tooth Apex Radius r (mm)	Tooth Front Angle α_1 (º)	Radius at Drilling tool Joint R (mm)
1	0.3	0.5	30	66.7 (101.6 Drilling tool)
2	0.6	1.0	40	79.4 (114.3 Drilling tool)
3	0.9	1.5	50	84.15 (127 Drilling tool)
4	1.2	2.0	60	88.9 (139.7 Drilling tool)

The orthogonal experimental method can effectively reduce the number of experiments and result in a more uniform data distribution. Finally, the data results are summarized and analyzed using the range analysis method or analysis of variance, leading to reliable conclusions. The experimental arrangement of an orthogonal experiment is typically expressed in the form of an orthogonal table. In an experiment

involving four factors, each with four levels, the standard orthogonal table chosen is $L_{16}(4^4)$. Here, L represents the orthogonal table code, 16 is the number of experiments, and 4 represents the number of levels for each factor. The experimental plan and results of the orthogonal experiment are shown in Table 2.

Table 2. Orthogonal Experiment Plan and Results

Experiment No.	t (mm)	r (mm)	α_1 (°)	R (mm)	Results
1	1	1	1	1	0.8720
2	1	2	2	3	0.8983
3	1	3	3	2	0.9270
4	1	4	4	4	0.9550
5	2	1	3	3	0.9271
6	2	2	4	1	0.9545
7	2	3	1	4	0.8716
8	2	4	2	2	0.8976
9	3	1	2	4	0.8981
10	3	2	1	2	0.8716
11	3	3	4	3	0.9543
12	3	4	3	1	0.9259
13	4	1	4	2	0.9540
14	4	2	3	4	0.9264
15	4	3	2	1	0.8971
16	4	4	1	3	0.8711

After calculating the experimental results, it is necessary to perform a comparative analysis of the results and summarize the conclusions. This paper uses the range analysis method to analyze the orthogonal experimental results. The range analysis method, as a simple and intuitive statistical analysis technique, evaluates the impact of different factors on the experimental results by calculating the range of the average values of the experimental results corresponding to each level. It can quickly reveal the significance of the impact of different factors on the experimental outcomes. The range analysis results of the orthogonal experiment are shown in Table 3.

Table 3. Orthogonal Experiment Range Analysis Table

Factors	1 Average	2 Average	3 Average	4 Average	Range
Bite Depth	0.9131	0.9127	0.9125	0.9122	0.0009
Tooth Apex Radius	0.9128	0.9127	0.9125	0.9124	0.0004
Tooth Front Angle	0.8716	0.8978	0.9266	0.9545	0.0829
Radius at Drilling tool Joint	0.9124	0.9126	0.9127	0.9128	0.0004

From Table 3, it can be seen that the range of the average experimental results corresponding to different levels of the tooth front angle α_1 is much larger than the range values of the other three factors. Therefore, the tooth front angle α_1 has the most significant impact on the equivalent coefficient of friction f_v, followed by the bite depth t. The effects of the tooth apex radius r and the radius at the drilling tool joint R on the equivalent coefficient of friction f_v are the smallest. The 3D surface plot of the mean equivalent friction coefficient f_v at the four levels of the four factors is shown in Figure 6.

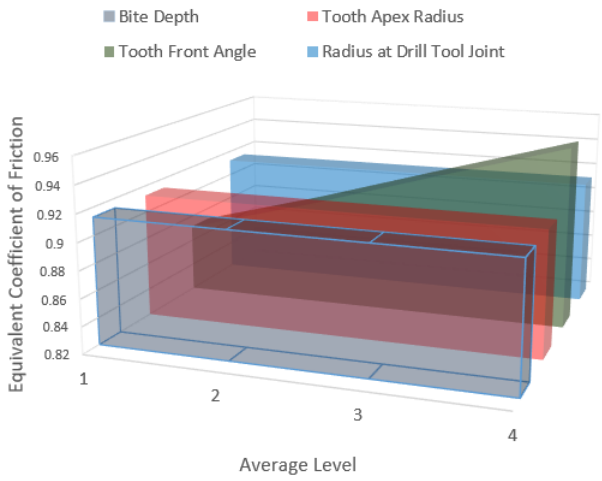

Figure 6. Mean Equivalent Friction Coefficient at Different Levels of the Four Factors

Based on Table 3 and Figure 6, it can be concluded that when designing the tong die, the tooth front angle α_1 and the tooth apex radius r need to be calculated and analyzed. Among these, the tooth front angle α_1 is the primary influencing factor. Within a certain range, the equivalent friction coefficient f_v increases as the tooth front angle α_1 increases. However, when the tooth height and tooth pitch are fixed, increasing the tooth front angle α_1 will cause the tooth pitch to increase, the number of teeth to decrease, and the tangential force on each tong die to increase, which can lead to failure. Therefore, the tooth front angle α_1 should not be too high, with the optimal range being between 35° and 45°. Since the tooth apex radius r has a very minimal effect on the equivalent friction coefficient f_v, it is considered a secondary factor.

6. Tong Die Simulation Experiment Analysis

The tong die directly contacts the drilling tool, and due to the large clamping force, the mechanical environment at the tooth tip is complex. Analyzing the mechanical performance of the tong die is therefore necessary. In the previous discussion, the optimal range for the tooth front angle was determined to be between 35° and 45°, based on the equivalent friction coefficient and tangential force. Since make-up and break-out are inverse processes, the tooth front angle and tooth back angle are equal. Therefore, the tooth apex angle range is 70° to 90°. For tooth apex angles of 70°, 80°, and 90°, corresponding tooth apex radii are 0.9 mm, 1.0 mm, and 1.1 mm, respectively. Finite element analysis of the tong dies gripping ϕ216 drilling tool was carried out for these three parameters. During the simulation, the primary focus was on studying the stress distribution when the tong die surface contacts the drilling tool. Since the tong die is in a compression state, the total deformation of the tong die is very small, so this aspect was not analyzed.

Figure 7 is stress distribution diagram of the tong die with 70° Tooth Apex Angle, and the stress distribution on the left and right tong dies is shown in Figure 7a and Figure 7b, respectively. Among them, the maximum stress on the left tong die is 1141 MPa, and the maximum stress on the right tong die is 1145 MPa.

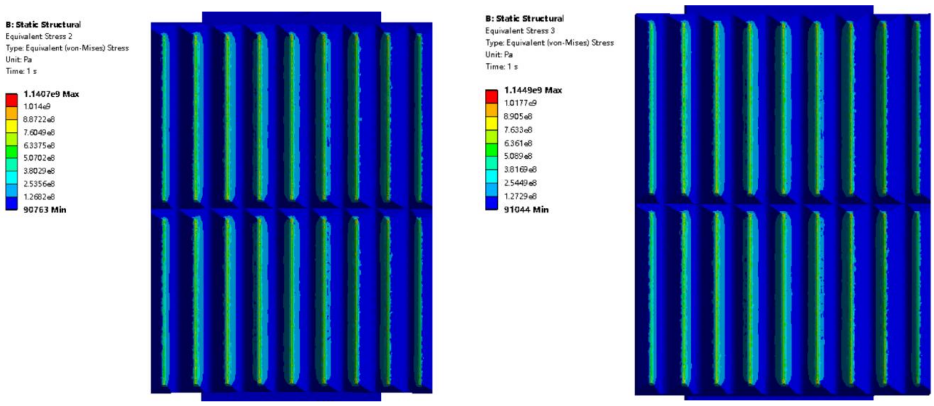

(a) (b)

Figure 7. Stress Distribution Diagram of the Tong Die with 70° Tooth Apex Angle. (a) Left Tong Die, (b) Right Tong Die

Figure 8 is stress distribution diagram of the tong die with 80° tooth apex angle, and the stress distribution on the left and right tong dies is shown in Figure 8a and Figure 8b, respectively. Among them, the maximum stress on the left tong die is 1331 MPa, and the maximum stress on the right tong die is 1277 MPa.

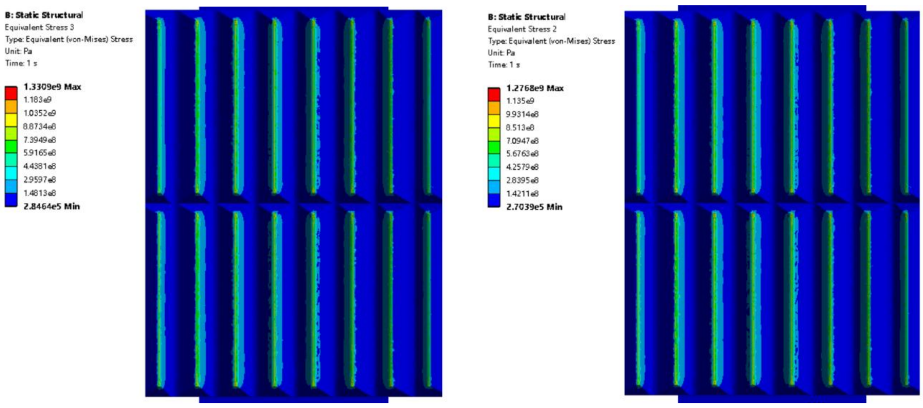

(a) (b)

Figure 8. Stress Distribution Diagram of the Tong Die with 80° Tooth Apex Angle. (a) Left Tong Die, (b) Right Tong Die

Figure 9 is stress distribution diagram of the tong die with 90° tooth apex angle, and the stress distribution on the left and right tong dies is shown in Figure 9a and Figure 9b, respectively. Among them, the maximum stress on the left tong die is 1581 MPa, and the maximum stress on the right tong die is 1584 MPa.

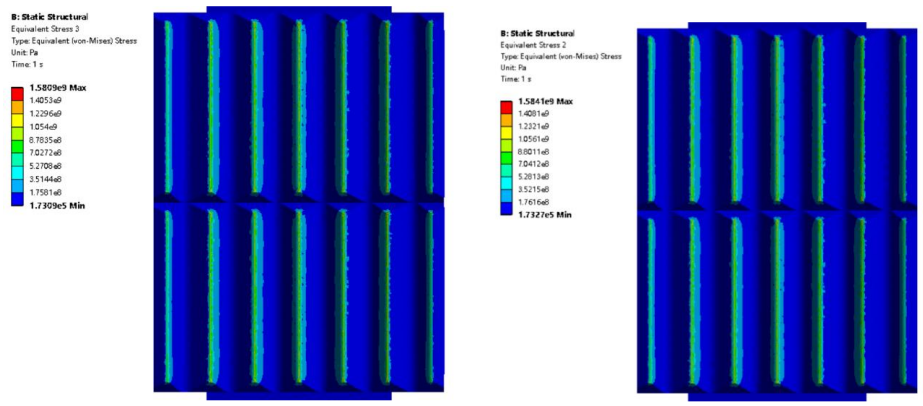

(a) (b)

Figure 9. Stress Distribution Diagram of the Tong Die with 90° Tooth Apex Angle. (a) Left Tong Die, (b) Right Tong Die

From Figure 7 to Figure 9, it can be seen that the stresses on the tong die for tooth apex angles of 70°, 80°, and 90° are mainly concentrated on the curved surface. Since the contact between the tong die and the drilling tool is a line contact, the maximum stress occurs at the tooth apex contact line. The stress distribution on the front and back faces of the tooth decreases as the distance from the contact line increases. The stress reduction rate on the front and back faces of the middle tong die is the same, meaning that the stress distribution on the front and back faces is identical. For the tong dies on both sides, the

stress on the tooth surface near the drilling tool's centerline is higher, while the stress on the surface farther from the centerline is lower.

Comparing the tong dies with different parameters, the stress values for the tong die with a 90° tooth apex angle are the highest, followed by the tong die with an 80° tooth apex angle, and the tong die with a 70° tooth apex angle has the lowest stress value. Moreover, the maximum stress values for all three tong dies exceed the yield limit of the tong die material, 20CrMnTi, which is 885 MPa, causing plastic deformation in the surface part of the tooth tip. This is considered normal. However, the tong die experiences stress singularities, and a stress equivalent linearization method is still required to verify the stress according to its type. The tong dies with 70° and 80° tooth apex angles meet the stress requirements, while the tong die with a 90° tooth apex angle has a local film stress that exceeds its allowable stress $1.5K\sigma_b$ (where K is the load combination factor, $K = 1$, and σ_b is the material yield strength). Considering the relationship between the tooth front angle and the equivalent friction coefficient, the 80° tooth apex angle is determined to be the best choice among the three parameters.

7. Conclusions

This paper is based on the issues faced by the tong dies of the clamping tong for the iron roughneck, and designs the clamping tong. The tong dies are studied from multiple perspectives such as tooth shape analysis, mechanical analysis, and contact condition analysis. The specific work and conclusions are as follows:

The paper introduces the structural composition of the clamping tong, and mechanical analysis of the tong die tooth profile angle is conducted, and a method for calculating the tong die height is derived.

An analysis of the contact conditions between the tong dies and the drilling tool is performed, and the equivalent coefficient of friction is calculated, along with the necessary conditions to prevent slippage. Additionally, the bite depth of the tong dies and the biting conditions are analyzed.

Through the orthogonal experimental method, the effects of various factors on the equivalent coefficient of friction are obtained. The results are analyzed using the range analysis method, and it is found that: the ranges of the tooth front angle, bite radius, tooth apex radius, and drilling tool joint radius are 0.0829, 0.0009, 0.0004, and 0.0004, respectively. This leads to the conclusion that the tooth front angle has the most significant effect on the equivalent coefficient of friction.

Based on the optimal range of the tooth apex angle derived from the equivalent coefficient of friction, experimental analysis is conducted on tong dies with 70°, 80°, and 90° tooth apex angles in the clamped drilling tool state. The stress distribution is obtained through simulation, and stress verification is carried out using the stress equivalent linearization method. The 80° tooth apex angle is determined to be the optimal choice.

Acknowledgement

This research was funded by Jilin Provincial Department of Science and Technology, grant number 20220201037GX.

References

Ba, S., Myers, W. R., & Brenneman, W. A. (2015). Optimal slice Latin hypercube design. *Technometrics*, *57*(4), 479-487. https://doi.org/10.1080/00401706.2014.957867

Guan, D., Yu, B., & Bi, J. (1998). Composition Type Teeth of Spider for Petroleum Borehole Drilling. *Chinese Patent CN2273764Y*. https://patents.google.com/patent/CN2273764Y

Hou, X. (2023). *Structural optimization and clamping capacity analysis of iron drill tong*. Xi'an Petroleum University.

Jiang, Q., & Zhang, D. (2003). Friction Type Tongs Teeth. *Chinese Patent CN2576421Y*. https://patents.google.com/patent/CN25764 21Y. 427

Li, Y., Cheng, G. G., Lu, J. L., et al. (2021). Effect of TiN precipitation on hardenability in 20CrMnTi gear steel. *Iron & Steel*, *56*(01), 75-84.

Luo, Z. (2018). *Key Technologies for the Design and Manufacture of Iron Drill Tong for Petroleum Drilling Rigs*. Chang'an University.

Pei, J., Song, C., Liu, Z., Chen, J., Shen, H., & Miao, H. (2019). Parameter analysis and optimization of iron drill tong teeth plate. *Journal of 432 Mechanical Strength*, *41*(05), 1096-1104. https://doi.org/10.16579/j.issn.1001.9669.2019.05.014

Sha, Y., Han, D., Chen, D., & Liu, C. (2024). Performance Analysis of New One-Piece Iron Roughneck and Its Spinning Mechanism. *Machines*, *12*(8), 575. https://doi.org/10.3390/machines12080575

Sun, Y., Zhang, F., Wang, Q., & Gao, K. (2016). Application of "Crust 1" 10k ultra-deep scientific drilling rig in Songliao Basin Drilling Project (CCSD-SKII). *Journal of Petroleum Science and Engineering*, *145*, 222-229. https://doi.org/10.1016/j.petrol.2016.04.003

Wang, M., Sun, S., Wang, H., Liu, Q., Zhang, H., Wang, Y., & Wang, J. (2019). *Orthogonal Experimental Study on Static Solution Assisted Laser Polishing of Stainless Steel*.

Wei, L. (2014). *Optimization design of key parameters for iron drill tong teeth*. Xi'an Petroleum University.

Xu, Z., Wang, L., Chen, G., Ma, Y., Yang, C., Xu, Y., Gong, X., & Tang, X. (2009). Non-marking Frictional Clamping Teeth. *Chinese Patent CN201292790Y*. https://patents.google.com/patent/CN201292790Y

Yan, W. H., Guo, L. T., Peng, Y., Duan, Z. Y., Wu, H., & Hu, N. (2019). Sensitivity analysis of iron drill tong parameters. *Journal of Xi'an Petroleum University (Natural Science Edition)*, *34*(05), 110-115.

Yang, L. Y., Li, W.W., & Cui, J. M. (2022). Sensitivity analysis of Duncan-Zhang E-B model parameters for dam deformation at different construction stages based on orthogonal experimental analysis. *Northwest Hydroelectric Power*, *02*, 76-80.

Zhang, K., Liu, Y., Jia, H., Yan, F., & Xue, G. (2023). Research on a Three-Dimensional Fuzzy Active Disturbance Rejection Controller for the Mechanical Arm of an Iron Roughneck. *Processes*, *11*(5), 1409. https://doi.org/10.3390/pr11051409

Zhou, H. C., Jin, C. Z., Zhang, W. R., & Liu, W. (2024). Experimental study on the surface roughness of machined 20CrMnTi steel in milling. *Manufacturing Technology and Machine Tools*, *01*, 80-84. https://doi.org/10.19287/j.mtmt.1005-2402.2024.01.011

Zhou, H. M., Hong, Y. C., Fu, X. J., Wang, W. J., & Zhang, C. X. (2021). Research on the optimization of hawthorn pigment extraction process using L16 (4-5) orthogonal experiment. *Modern Food*, *01*, 102-103+112. https://doi.org/10.16736/j.cnki.cn41-14 34/ts.2021.01.029